

Numerical Simulation of Pitch-Damping Dynamic Derivatives

*Yuanhong Ma**, *Meng Lv***, *Cheng Su****

China Academy of Aerospace Aerodynamics

No.17 Yungang Road, Fengtai, Beijing, China, 100074

**yuanhongma@163.com*

***lclmmk@163.com*

****Xiaoacheng@hotmail.com*

Abstract

The dynamic derivatives are used to describe the dynamic aerodynamic characteristics of flight vehicles when the maneuvering flight is disturbed, it is important in flight vehicles' design and dynamic characteristics analysis. The equations of forced oscillation and forced plunging motion of flight vehicles, and the expressions for calculating the identification of pitch-damping dynamic derivatives were derived. We simulated pitching and plunging of NACA0012 airfoil and basic finner missile. The results of simulation are consistent with the references.

1. Introduction

Aerodynamic stability parameters of an aircraft are mainly characterized by dynamic stability derivatives. They are measures of how the in-flight forces and moments acting on a flight body change in response to changes in flight states, such as angle of attack and velocity. The main dynamic stability derivatives contain the pitch damping force, pitch damping moment, roll damping moment, Magnus force and Magnus moment.

The traditional method analyzing the dynamic characteristics is wind tunnel test by using scaled model. Usually, the period of wind tunnel test is long and the research cost is high. Dynamic derivatives are generally difficult to obtain by experimental or theoretical means. Compared to numerical simulation, the wind tunnel test data has physical factuality, but it has a lot of limits, such as scaled dimensions, wind tunnel choking, support interferences, Reynolds number effects and so on. These problems make the characteristics of scaled models and real flight vehicles different. Currently, the computational fluid dynamic (CFD) numerical simulation by solving Navier-Stokes has achieved relatively nice level, which could solve complex flow on massively parallel processor with lower cost. CFD methods could remove interferences of wind tunnel and simulate the real flight test.

The pitch-damping combined and individual dynamic derivatives were obtained by CFD numerical simulation. An unsteady time-accurate Reynolds-Averaged Navier-Stokes (RANS) CFD techniques and linear flight mechanics theory were used to compute the pitch damping moments. These motions are time-dependent. In order to take into account the rotation of the computational domain, an Arbitrary Lagrangian Euler (ALE) formulation has been used. The velocity grid only results from the composition of a motion of translation and rotation and there is no time-varying cell volume. In the Navier-Stokes equations, the grid motion is taken into account by the rigid body technique. The mesh is moving, but not deforming. Grid velocity is assigned to each mesh point. The computation grids generated for this study are multi block structured grids building with ICEM. The pitch-damping combined dynamic derivatives were obtained by simulation of forced pitching oscillation of flight vehicle by rigid dynamic grid; the plunging derivatives were obtained by simulation of plunging of flight vehicle by rigid dynamic grid. We simulated pitching and plunging of NACA0012 airfoil and Basic Finner. The results of simulation are consistent with the references. In the future, it will be necessary to use more complex turbulence model to predict the onset of flow separation and the development of vortices.

2. Numerical methods

2.1 N-S Equations

The three-dimensional compressible integral N-S equation can be expressed as:

$$\iiint \frac{\partial \bar{Q}}{\partial t} d\Omega + \iiint \nabla \bar{F} d\Omega = \iiint \nabla \bar{F}_v d\Omega$$

$\bar{Q} = [\rho, \rho u, \rho v, \rho w, \rho E]^T$ are conserved variables, \bar{F} and \bar{F}_v are inviscid flux and viscous flux, their expression are:

$$\bar{F} = \begin{bmatrix} \rho u & \rho v & \rho w \\ \rho u^2 + p & \rho uv & \rho uw \\ \rho vu & \rho v^2 + p & \rho vw \\ \rho wu & \rho wv & \rho w^2 + p \\ \rho u(E + p/\rho) & \rho v(E + p/\rho) & \rho w(E + p/\rho) \end{bmatrix}$$

$$\bar{F}_v = \begin{bmatrix} 0 & 0 & 0 \\ \sigma_{xx} & \sigma_{xy} & \sigma_{xz} \\ \sigma_{xy} & \sigma_{yy} & \sigma_{yz} \\ \sigma_{xz} & \sigma_{yz} & \sigma_{zz} \\ \varphi_x & \varphi_y & \varphi_z \end{bmatrix}$$

$$\begin{bmatrix} \varphi_x \\ \varphi_y \\ \varphi_z \end{bmatrix} = \begin{bmatrix} \kappa \frac{\partial T}{\partial x} + u\sigma_{xx} + v\sigma_{xy} + w\sigma_{xz} \\ \kappa \frac{\partial T}{\partial y} + u\sigma_{xy} + v\sigma_{yy} + w\sigma_{yz} \\ \kappa \frac{\partial T}{\partial z} + u\sigma_{xz} + v\sigma_{yz} + w\sigma_{zz} \end{bmatrix}$$

2.2 Numerical methods of combined derivative

For forced pitching oscillation with a single degree of freedom, the simplified harmonic oscillation (dimensionless) is given as follows:

$$\alpha = \alpha_0 + \alpha_m \sin(kt) = \alpha_0 + \theta$$

α_0 is initial angle of attack, α_m is amplitude, $k = \omega L_{ref} / 2V_\infty$ is reduction frequency.

By using the integral method, the solution formula of combined derivative is:

$$C_{mq} + C_{m\dot{\alpha}} = \frac{1}{ka_m^2 \pi} \oint C_m d\alpha$$

2.3 Numerical methods of the time difference derivative

The sinusoidal motion of a forced aircraft is governed by the following law:

$$z(t) = z_m \sin(kt)$$

z_m is the amplitude of plunging motion.

Similarly, the integral method can be used to obtain the formula for calculating the time difference derivative of small-amplitude plunging motion:

$$C_{m\dot{\alpha}} = \frac{V_\infty^2}{\pi z_m^2 k^3} \oint C_m d\alpha$$

3. Numerical simulation results and analysis

3.1 NACA0012 airfoil pitching motion numerical simulation

The NACA0012 airfoil small-amplitude pitching motion test ^[1] reported in AGARD-R-702 is widely used in pitching motion dynamic tests and CFD dynamic calculation verifications. In this paper, the same flow conditions as the experiments are adopted:

$$Ma = 0.755, Re = 5.5 \times 10^6, \alpha_0 = 0.016^\circ, k=0.0814, \alpha_m = 2.51^\circ.$$

Figure 1 and Figure 2 are the hysteresis curves of lift coefficients and pitching moment coefficients with angles of attack. It can be seen that the calculated results are close to the experimental results, which shows that the simulation results in this paper are reliable.

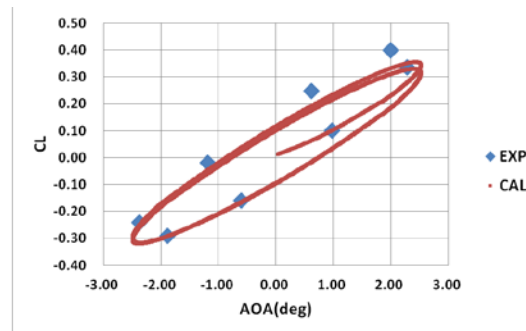


Figure 1: Lift coefficients varying with angles of attack comparing to experimental results

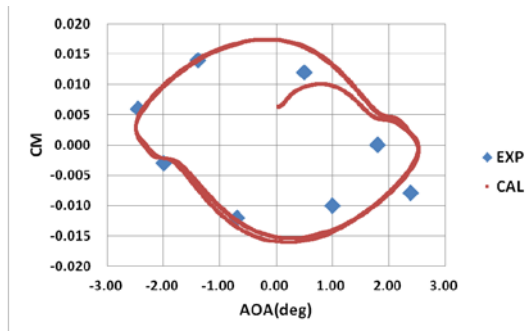


Figure 2: Pitching moment coefficients varying with angles of attack comparing to experimental results

3.2 NACA0012 airfoil plunging motion numerical simulation

Plunging motion of NACA0012 airfoil is an example in CFD++ Help Manual ^[2]. The same flow conditions are adopted:

$$Ma = 0.3, Re = 5.5 \times 10^6, \alpha = 0^\circ$$

Amplitude is 3.21 m, $f = 0.2653$ Hz. Plunging motion is in accordance with sinusoidal law. Figure 3 and Figure 4 are the curves of normal force coefficients and pitching moment coefficients. Comparing the results calculated in this paper and CFD++, it can be seen that the difference between them is small, which shows that the simulation of plunging motion in this paper is reliable.

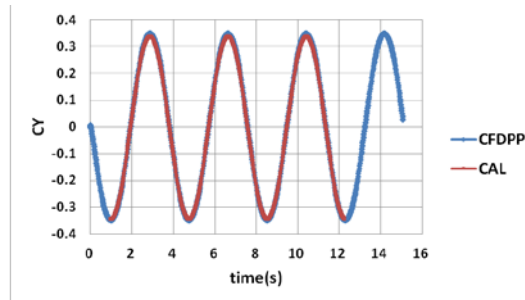


Figure 3: Normal force coefficients varying with time

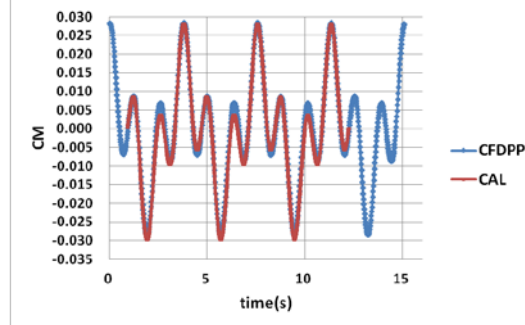


Figure 4: Pitching moment coefficients varying with time

3.3 Basic finner pitching motion numerical simulation

Small-amplitude pitching motion and the same flow conditions as the experiments^[3] are adopted:

$Ma = 1.96$, $Re = 5.89 \times 10^6$, $\alpha_0 = 0^\circ, 2.5^\circ, 4^\circ, 5^\circ, 10^\circ, 15^\circ, 20^\circ, 25^\circ, 30^\circ$, $k=0.01$, $\alpha_m = 1^\circ$. Figure 5 is the comparison between experiments and calculations. It shows that the results of calculations are reliable.

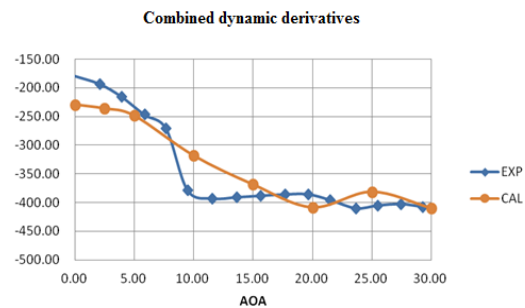


Figure 5: Combined dynamic derivatives varying with angles of attack comparing to experimental results

3.4 Basic finner plunging motion numerical simulation

Small-amplitude plunging motion and the same flow conditions as the references^{[4][5]} are adopted:

$Ma = 1.96$, $Re = 5.89 \times 10^6$, $\alpha_0 = 0^\circ, 2.5^\circ, 5^\circ, 10^\circ, 15^\circ, 20^\circ, 25^\circ, 30^\circ$, $k=0.01$, $z_m = 0.03m$. Figure 6 is the comparison between references and calculations. It shows that the results of calculations are reliable.

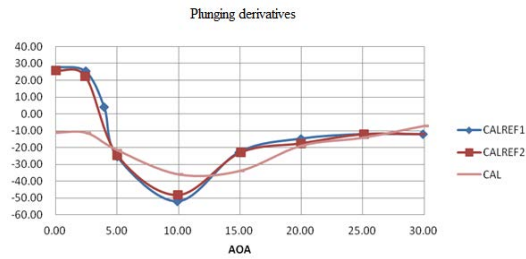


Figure 6: Plunging derivatives varying with angles of attack comparing to references

3. Conclusions

We simulated pitching and plunging of NACA0012 airfoil and Basic Finner. The results of simulation are consistent with the references. In the future, it will be necessary to use more complex turbulence model to predict the onset of flow separation and the development of vortices.

References

- [1] Landon, R. H. NACA 0012 oscillatory and transient pitching [R]. AGARD Report 702, Compendium of unsteady aerodynamics measurements. 1982
- [2] METACOMP. CFD++ user manual.
- [3] Uselton, et al. Test Mechanism for Measuring Pitch-Damping Derivatives of Missile Configurations at High Angles of Attack. 1975.
- [4] XI Ke, YAN Chao, HUANG Yu, et al. Numerical Simulation of individual compenents of pitch-damping coefficient sum. Journal of Beijing University of Aeronautics and Astronautics. 2015
- [5] MI Baigang, ZHAN Hao. New Calculation Methods for Dynamic Derivatives of Advanced Flight Vehicles. Journal of Shanghai Jiao Tong University. 2016